CONF-860715--2

LA-UR -86-3265

Los Alamos National Laboratory is operated by the University of California for the United States Department of Energy under contract W-7405-ENG-36

LA-UR--86-3265

DE87 000160

TITLE: MECHANISM OF NUCLEAR DISSIPATION IN FISSION AND HEAVY-ION REACTIONS

AUTHOR(S): J. R. Nix and A. J. Sierk

SUBMITTED TO: For presentation at the International School-Seminar on Heavy Ion Physics, Dubna, USSR, September 23-30, 1986

DISCLAIMER

Los Alamos Los Alamos National Laboratory
Los Alamos, New Mexico 87545

FORM NO 836 R4
ST NO 2629 5/81

MECHANISM OF NUCLEAR DISSIPATION IN FISSION AND HEAVY-ION REACTIONS

J. R. Nix and A. J. Sierk
Theoretical Division, Los Alamos National Laboratory

Abstract

We review recent advances in our theoretical understanding of nuclear dissipation at intermediate excitation energies, with particular emphasis on a new surface-plus-window mechanism that involves interactions of either one or two nucleons with the moving nuclear surface and also, for dumbbell-like shapes encountered in fission and heavy-ion reactions, the transfer of nucleons through the window separating the two portions of the system. This novel dissipation mechanism provides a unified macroscopic description of such diverse phenomena as widths of isoscalar giant quadrupole and giant octupole resonances, mean fission-fragment kinetic energies and excitation energies, dynamical thresholds for compound-nucleus formation, enhancement in neutron emission prior to fission, and widths of mass and charge distributions in deep-inelastic heavy-ion reactions.

1. Introduction

For many years the Dubna school-seminars have provided an important forum for the introduction of new ideas to the scientific world. Your 1975 school-seminar, in which we had the pleasure of participating,[1] was instrumental in stressing the role played by nuclear dynamics on the production of heavy nuclei, and represented a turning point in our view concerning the mechanism and magnitude of nuclear dissipation.[1,2]

Previously, it had been believed that the mechanism of nuclear dissipation is two-body collisions, like that responsible for ordinary viscosity in fluids, and that the magnitude is sufficiently small that nuclei are mobile, like mercury.[3] But then it was realized that the long mean free path of nucleons inside a nucleus, arising from the Pauli exclusion principle for fermions, alters both the mechanism and magnitude.[2,4,5] However, the subsequent approximations made in incorporating this single physical principle have led to radically different pictures.

By assuming that the velocity distribution of nucleons striking a moving container wall is completely random, Swiatecki and his colleagues derived and first presented to the 1975 school-seminar a simple wall formula for describing such one-body dissipation, in terms of which nuclei are predicted to be superviscid.[2,6–12] We will be hearing an update on this point of view at this school-seminar by Błocki.[13] In contrast, by constraining the many-body wave function to at all times be a Slater determinant of single-particle wave functions, Bonche, Davies, Koonin, Negele and others treated the dynamics by use of the time-dependent Hartree-Fock approximation, in terms of which nuclei dissipate much less energy.[14–16] Attempts to experimentally discriminate between such possibilities have thus far proved elusive because of the difficulty of distinguishing dissipative effects from analogous effects caused by collective degrees of freedor

2. Surface-plus-Window Dissipation

We present here a new macroscopic approach to this problem, valid for intermediate excitation energies above which pairing has disappeared and below which the nucleon mean free path exceeds the nuclear diameter. For such excitation energies, the dissipation proceeds primarily in the surface region from two distinct mechanisms. The first mechanism is one-body dissipation, but with a magnitude that is substantially reduced relative to that of the wall formula. In calculations based on the random-phase approximation for spherical nuclei, Griffin, Dworzecka, and Yannouleas have shown that the effect of replacing three idealizations of the wall formula by more realistic features appropriate to real nuclei is to reduce the one-body dissipation coefficient to roughly 10% of the wall-formula value.[17,18] Alternatively, the reduction could arise because the nucleons retain some memory of their previous collisions with the wall, which invalidates the assumption of a random velocity distribution that was used to derive the wall formula. The second mechanism is two-body collisions in the surface region. The Pauli exclusion principle, which suppresses two-body collisions in the nuclear interior, disappears as one passes through the nuclear surface to the exterior.[19] Since the density decreases to zero outside the nucleus, the probability for two-body collisions peaks in the nuclear surface.

We assume that the surface dissipation is local and calculate it from the leading term in an expansion of the time rate of change of the collective Hamiltonian H in powers of the surface diffuseness divided by the nuclear radius.[8] We write this leading term as

$$\left(\frac{dH}{dt}\right)_{\text{surface}} = -k_s \rho \bar{v} \int (\dot{n} - D)^2 dS \ , \tag{1}$$

were $\dot{n}$ is the velocity of a surface element dS, D is the normal drift velocity of nucleons about to strike the surface element dS, $\bar{v}$ is the average speed of the nucleons inside the nucleus, ρ is the nuclear mass density, and k_s is a dimensionless parameter that specifies the total strength of the interaction of either one or two nucleons with the moving nuclear surface. A value of $k_s = 1$ would correspond to the wall formula, but several types of experimental data indicate that for real nuclei its value is much less than unity. In principle, the value of k_s could depend upon both the excitation energy and type of collective motion involved. Our approach here is to assume a single value of k_s and then determine, from comparisons with experimental data, whether or not this single value is appropriate to the range of intermediate excitation energies and variety of collective phenomena under consideration.

For dumbbell-like shapes, the transfer of nucleons through the window separating the two portions of the system leads to an additional dissipation that is analogous to the classical window formula of Swiatecki.[2,6-12] Our result is

$$\left(\frac{dH}{dt}\right)_{\text{window}} = -\frac{1}{2}\rho \bar{v} a \dot{r}^2 F(q, \dot{q}) \ , \tag{2}$$

where a is the area of the window, $\dot{r}$ is the relative velocity of the centers of mass of the two portions of the system, and $F(q, \dot{q})$ describes the effect of a nonuniform velocity as a function of position in the deforming fragments. There is no need to renormalize this part of the dissipation because nucleons that have passed through a small window have a low probability of returning through it while still retaining memory of their previous passage.

The combination of these two mechanisms leads to surface-plus-window dissipation. In calculating the total dissipation rate dH/dt, we describe the transition from the pure surface dissipation that applies to mononuclear shapes, where the drift D is zero in Eq. (1), to the surface-plus-window dissipation that applies to dinuclear shapes, where the drift D is nonzero in Eq. (1), by use of a smooth interpolation analogous to that used in Ref. 20.

3. Giant-Resonance Widths

As the first application of our new dissipation picture, we calculate the isoscalar giant-resonance width as a function of mass number A and multipole degree n. We approximate such resonances by small-amplitude collective oscillations in which the neutrons and protons undergo in-phase, incompressible, irrotational flow with unit effective mass.[21] This type of flow pattern is expected to arise when the nucleons remain in orbitals characterized by their original nodal structure.

With the radius vector to the nuclear surface expanded in a series of Legendre polynomials $P_n(\cos\theta)$, the expansion coefficients α_n satisfy the equations of motion

$$M_n\ddot{\alpha}_n + \eta_n\dot{\alpha}_n + C_n\alpha_n = 0 \ , \tag{3}$$

where M_n is the inertia, η_n is the dissipation coefficient, and C_n is the stiffness coefficient for the distortion of degree n. The inertia is given by[21]

$$M_n = \frac{3}{n(2n+1)}M_0R_0^2 \ , \tag{4}$$

where

$$M_0 = mA \tag{5}$$

is the total mass of the nucleus and

$$R_0 = r_0A^{1/3} \tag{6}$$

is the equivalent sharp radius of the spherical nucleus. The dissipation coefficient is obtained by evaluating Eq. (1) with $D = 0$, which leads to

$$\eta_n = -\frac{1}{\dot{\alpha}_n^2}\left(\frac{dH}{dt}\right)_{\text{surface}} = \frac{4\pi}{(2n+1)}k_s\rho\bar{v}R_0^4 \ . \tag{7}$$

The width for a giant resonance of multipole degree n is then given by

$$\Gamma_n = \hbar\eta_n/M_n = \hbar k_s\bar{v}n/R_0 = \frac{3(9\pi)^{1/3}\hbar^2k_sn}{8mr_0^3A^{1/3}} \ , \tag{8}$$

where we have used the relationship $\bar{v} = \frac{3}{4}v_F$ and inserted the usual result for the Fermi velocity v_F. Three of the constants that appear in Eq. (8) have values that are already well determined, and for these we use[22,23]

$$r_0 = 1.16 \text{ fm} \ , \tag{9}$$

$$\hbar = 197.32858 \text{ MeV}/c \ , \tag{10}$$

and

$$m = 931.5016 \text{ MeV}/c^2 \ , \tag{11}$$

where c is the speed of light. For the value of the remaining parameter k_s, we find

$$k_s = 0.27 \tag{12}$$

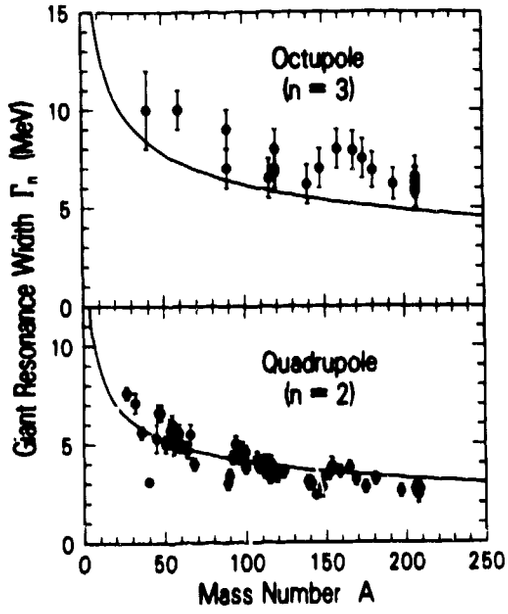

Fig. 1. Simultaneous reproduction of experimental isoscalar giant quadrupole and giant octupole widths by surface dissipation.

by adjustment to experimental widths of isoscalar giant quadrupole and giant octupole resonances./[24]/ Insertion of these values into Eq. (8) leads to

$$\Gamma_n = 9.58 n A^{-1/3} \text{ MeV} \ . \tag{13}$$

The solid curves in Fig. 1 give the results of this simple prediction for $n = 2$ and 3, corresponding to quadrupole and octupole resonances, respectively. Upon comparing the curves with the experimental widths that are also included in Fig. 1, we see that our new dissipation picture satisfactorily reproduces the average trends of the experimental widths with respect to both mass number A and multipole degree n, although the experimental octupole widths are systematically somewhat higher than the calculated curve. This discrepancy could arise from residual two-particle collisions in the nuclear interior, since for ordinary two-body viscosity the predicted ratio of the octupole to quadrupole width/[21]/ is 2.8, compared to 1.5 for surface dissipation. Such collisions in the nuclear interior could also affect somewhat the dependence of the width upon mass number, since two-body viscosity leads to an $A^{-2/3}$ dependence,/[21]/ compared to an $A^{-1/3}$ dependence for surface dissipation.

4. Macroscopic-Microscopic Method

For the treatment of the large distortions that are involved in fission and heavy-ion reactions, we focus from the outset on those few collective coordinates that are most relevant. In particular, for a system of A nucleons, we separate the $3A$ degrees of freedom representing their center-of-mass motion into N collective degrees of freedom that are treated explicitly and $3A - N$ internal degrees of freedom that are treated implicitly.

We specialize to axially symmetric nuclear shapes and describe them in cylindrical coordinates by means of the Legendre polynomial expansion/[25]/

$$\rho_s^2(z) = R_0^2 \sum_{n=0}^{N} q_n P_n[(z - \bar{z})/z_0] \ . \tag{14}$$

In this expression, z is the coordinate along the symmetry axis, ρ_s is the value on the surface of the coordinate perpendicular to the symmetry axis, z_0 is one-half the distance between the two ends of the shape, $\bar{z}$ is the value of z at the midpoint between the two ends, R_0 is the radius of the spherical nucleus, P_n is a Legendre polynomial of degree n, and q_n for $n \neq 0$ and 1 are $N-1$ shape coordinates. Since the nucleus is assumed to be incompressible, the quantity q_0 is not independent but is instead determined by volume conservation. Also, q_1 is determined by fixing the center of mass. In addition, we include an angular coordinate $\Theta \equiv q_{N+1}$ to describe the rotation of the nuclear symmetry axis in the reaction plane, which leads to a total of N collective coordinates $q = q_2, \ldots, q_{N+1}$ that are considered. Throughout this paper we use $N = 11$, corresponding to five independent symmetric and five independent asymmetric shape coordinates and one angular coordinate.

We consider excitation energies that are sufficiently high that single-particle effects may be neglected and calculate the potential energy of deformation $V(q)$ as the sum of repulsive Coulomb and centrifugal energies and an attractive Yukawa-plus-exponential potential,[26] with constants determined in a recent nuclear mass formula.[22] This generalized surface energy takes into account the reduction in energy arising from the nonzero range of the nuclear force in such a way that saturation is ensured when two semi-infinite slabs are brought into contact.

The collective kinetic energy is given by

$$T = \frac{1}{2} M_{ij}(q)\dot{q}_i\dot{q}_j = \frac{1}{2}[M(q)^{-1}]_{ij}p_ip_j \quad , \tag{15}$$

where the collective momenta p are related to the collective velocities $\dot{q}$ by

$$p_i = M_{ij}(q)\dot{q}_j \quad . \tag{16}$$

In these equations and the remainder of this paper we use the convention that repeated indices are to be summed over from 2 to $N+1$. At the high excitation energies and large deformations considered here, where pairing correlations have disappeared and near crossings of single-particle levels have become less frequent, the rotational moment of inertia is close to the rigid-body value and the vibrational inertia is close to the incompressible, irrotational value.[27] We therefore calculate the inertia tensor $M(q)$, which is a function of the shape of the system, for a superposition of rigid-body rotation and incompressible, nearly irrotational flow. For this purpose we use the Werner-Wheeler method, which determines the flow in terms of circular layers of fluid.[28]

The coupling between the collective and internal degrees of freedom gives rise to a dissipative force whose mean component in the ith direction may be written as

$$F_i = \frac{1}{2}\frac{\partial}{\partial \dot{q}_i}\left(\frac{dH}{dt}\right) = -\eta_{ij}(q)\dot{q}_j = -\eta_{ij}(q)[M(q)^{-1}]_{jk}p_k \quad . \tag{17}$$

The shape-dependent dissipation tensor $\eta(q)$ that describes the conversion of collective energy into single-particle excitation energy is calculated primarily for our new surface-plus-window model that was described in Sec. 2. However, we will also consider in Sec. 6 wall-and-window dissipation, which is obtained by setting $k_s = 1$ in Eq. (1).

In addition to the mean dissipative force, the coupling between the collective and internal degrees of freedom gives rise to a residual fluctuating force, which we treat under the Markovian assumption that it does not depend upon the system's previous history. At high excitation energies, where classical statistical mechanics is valid, we are led to the generalized Fokker-Planck equation

$$\frac{\partial f}{\partial t} + (M^{-1})_{ij} p_j \frac{\partial f}{\partial q_i} - \left[\frac{\partial V}{\partial q_i} + \frac{1}{2} \frac{\partial (M^{-1})_{jk}}{\partial q_i} p_j p_k \right] \frac{\partial f}{\partial p_i}$$

$$= \eta_{ij} (M^{-1})_{jk} \frac{\partial}{\partial p_i} (p_k f) + \tau \eta_{ij} \frac{\partial^2 f}{\partial p_i \partial p_j} \tag{18}$$

for the dependence upon time t of the distribution function $f(q, p, t)$ in phase space of collective coordinates and momenta. The last term on the right-hand side of this equation describes the spreading of the distribution function in phase space, with a rate that is proportional to the dissipation strength and the nuclear temperature τ, which is measured here in energy units.

Equation (18) has been solved recently for three important special cases. First, an analytical solution for the mean saddle-to-scission time has been obtained from a one-dimensional stationary Fokker-Planck equation.[29] Second, a numerical solution for the transient time required to build up the quasi-stationary probability flow over the fission barrier has been obtained from a one-dimensional time-dependent Fokker-Planck equation.[30] Third, a numerical solution for the fission-fragment kinetic-energy distribution has been obtained from a two-dimensional time-dependent Fokker-Planck equation.[31]

Except for such special cases, it is still difficult in practice to solve the generalized Fokker-Planck equation. Therefore, in most of our studies we use equations for the time rate of change of the first moments of the distribution function, with the neglect of higher moments. These are the generalized Hamilton equations

$$\dot{q}_i = (M^{-1})_{ij} p_j \tag{19}$$

and

$$\dot{p}_i = -\frac{\partial V}{\partial q_i} - \frac{1}{2} \frac{\partial (M^{-1})_{jk}}{\partial q_i} p_j p_k - \eta_{ij} (M^{-1})_{jk} p_k \ , \tag{20}$$

which we solve numerically for each of the N generalized coordinates and momenta.

5. Fission

We show in Fig. 2 how our new surface-plus-window dissipation, with strength $k_s = 0.27$, slows down the dynamical evolution of an excited ^{240}Pu nucleus compared to that for no dissipation. The initial conditions at the fission saddle point incorporate the effect of dissipation on the fission direction and are calculated for a nuclear temperature of 2 MeV by determining the average speed of all nuclei that pass per unit time through the saddle point with positive velocity.[29] Compared to the values for no dissipation, surface-plus-window dissipation increases the time from the saddle point to a zero-neck-radius scission point from 2.6×10^{-21} s to 8.4×10^{-21} s, and decreases the translational kinetic energy at scission from 50.0 MeV to 11.7 MeV. Leading to a scission shape that is more compact than that for no dissipation, surface-plus-window dissiption gives 28.9 MeV of dissipated energy during the dynamical descent from saddle to scission.

We treat the post-scission dynamical motion in terms of two spheroids, with initial conditions determined by keeping continuous the values of two shape moments and their time derivatives. Surface-plus-window dissipation reduces the average fission-fragment translational kinetic energy at infinity from 193.6 MeV for no dissipation to 176.7 MeV.

Our calculated average kinetic energies for the fission of nuclei throughout the periodic table, with the atomic number Z related to the mass number A according to Green's approximation to

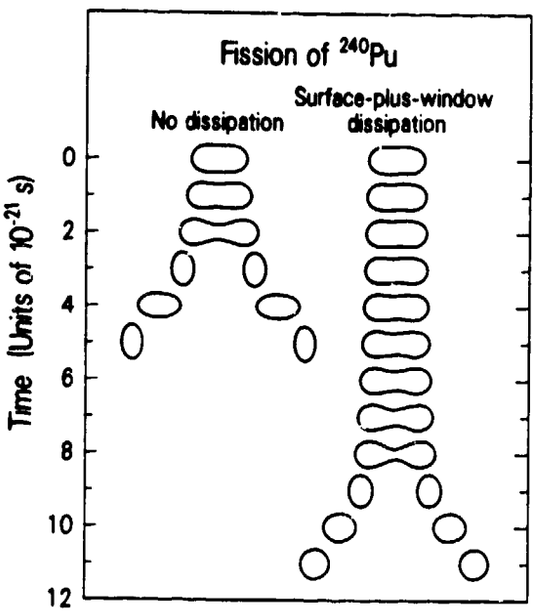

Fig. 2. Effect of surface-plus-window dissipation on the dynamical evolution of ^{240}Pu beyond its fission saddle point, for a nuclear temperature of 2 MeV.

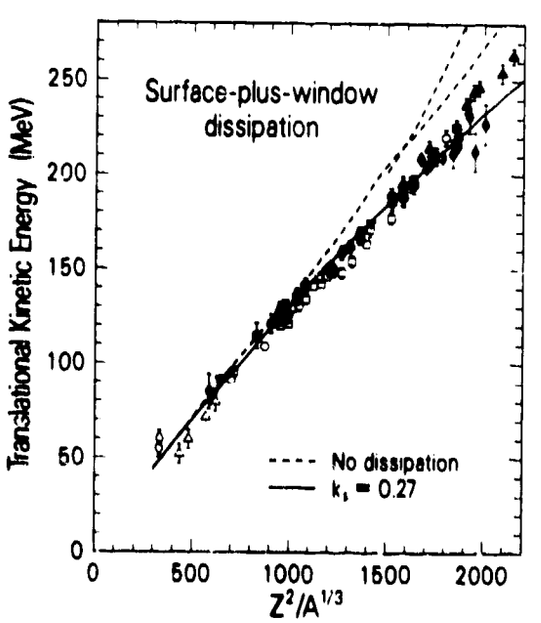

Fig. 3. Reduction of average fission-fragment kinetic energies by surface-plus-window dissipation, compared to experimental values.

the valley of beta stability,[32] are shown in Fig. 3 for a nuclear temperature of 2 MeV. When compared with experimental values for the fission of nuclei at high excitation energy,[20] where single-particle effects have decreased in importance, the dashed curves calculated with no dissipation are for heavy nuclei substantially higher. The presence of two dashed curves for $Z^2/A^{1/3} \geq 1500$ results from our use of two different approximations for treating the post-scission motion when a third fragment has formed between the two end fragments.[20] The solid curve, calculated with our new surface-plus-window dissipation with a strength previously determined from the widths of isoscalar giant resonances, satisfactorily reproduces the experimental data, although it lies slightly above some of the data for $Z^2/A^{1/3} \approx 1300$ and slightly below for $Z^2/A^{1/3} \geq 1900$. These small discrepancies could be associated with effects arising from the rupture of the neck prior to its reaching a zero radius, as is currently required in our calculations.

6. Heavy-Ion Reactions

Already at the 1975 Dubna school-seminar, it had been recognized that a necessary condition for forming a compound nucleus is that the dynamical trajectory for the fusing system pass inside the fission saddle point in a multidimensional space.[1] The dynamical trajectories and hence the cross sections for forming a compound nucleus depend strongly upon the location of the fission saddle point relative to the contact point. For light nuclear systems the fission saddle point lies outside the contact point, so that all of the angular-momentum states that cross the one-dimensional interaction barrier automatically pass inside the saddle point. However, for heavy nuclear systems and/or large impact parameters, the fission saddle point lies inside the contact point, and the center-of-mass bombarding energy must exceed the maximum in the one-dimensional zero-angular-momentum interaction barrier by an amount ΔE in order to form a compound nucleus. This additional bombarding energy ΔE has been calculated over the past 13 years by use of various approximations and for several dissipation mechanisms.[1,9,10,12,13,20,33–35] Here we concentrate on results that we have just obtained by solving Eqs. (19) and (20) numerically for our new surface-plus-window mechanism, as well as for no dissipation and wall-and-window dissipation.

The initial growth of the neck that forms between the approaching target and projectile corresponds primarily to a geometrical overlap of the tails of their density distributions rather than to a dynamical flow of matter. Therefore, we do not begin our numerical integrations of Eqs. (19) and (20) until the equivalent-sharp-surface neck radius has grown to 3 fm. Prior to this, we treat the target and projectile as rigid spheres and calculate any dissipation that is present by use of Randrup's proximity formalism.[36] Although we have studied the effect of using targets and projectiles away from the valley of beta stability, the results presented here are all calculated for systems in which the target and projectile each lie along Green's approximation to the valley of beta stability.[32]

As an example of our results for symmetric systems, we select the compound system with $Z^2/A = 39.5$, for which the fission saddle point for zero angular momentum lies somewhat inside the contact point. Figures 4 and 5 show the calculated shapes and trajectories, respectively, for the critical bombarding energy for each dissipation that is just sufficient to drive the system inside the fission saddle point. The additional bombarding energy ΔE that labels each result is measured relative to the maximum in the zero-angular-momentum interaction barrier calculated for spherical nuclei by use of the Yukawa-plus-exponential potential,[26] with constants determined in a recent nuclear mass formula.[22] The trajectories in Fig. 5 are plotted as functions of the two most important symmetric moments characterizing the shape. The moment r is the distance between the centers of mass of the two portions of the system, and the moment σ is the sum of

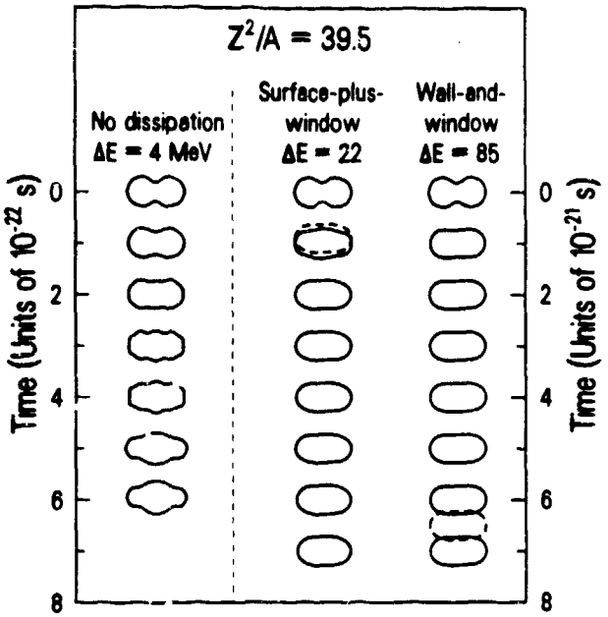

Fig. 4. Effect of dissipation on the dynamical evolution of $^{106.6}45.9 + {}^{106.6}45.9 \rightarrow {}^{213.2}91.8$ at zero impact parameter and bombarding energy in each case that is just sufficient to form a compound nucleus. The fission saddle-point shape is shown dashed in each of the two right-hand columns at the times when the trajectories pass closest to it.

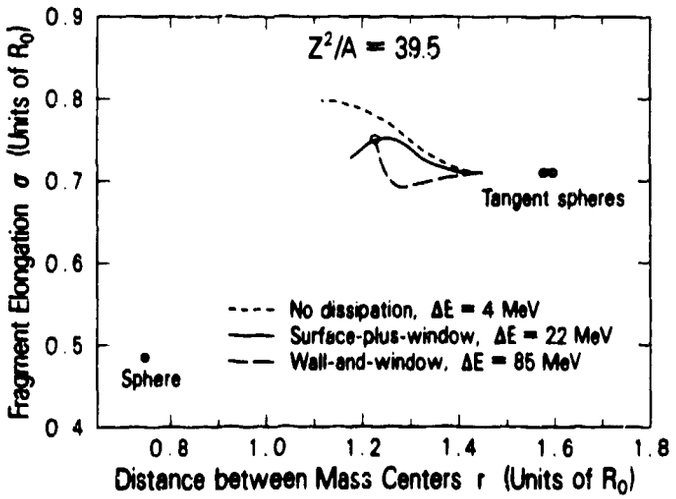

Fig. 5. Effect of dissipation on the dynamical trajectories for $^{106.6}45.9 + {}^{106.6}45.9 \rightarrow {}^{213.2}91.8$ at zero impact parameter and bombarding energy in each case that is just sufficient to form a compound nucleus. The fission saddle point is located at the position of the open point.

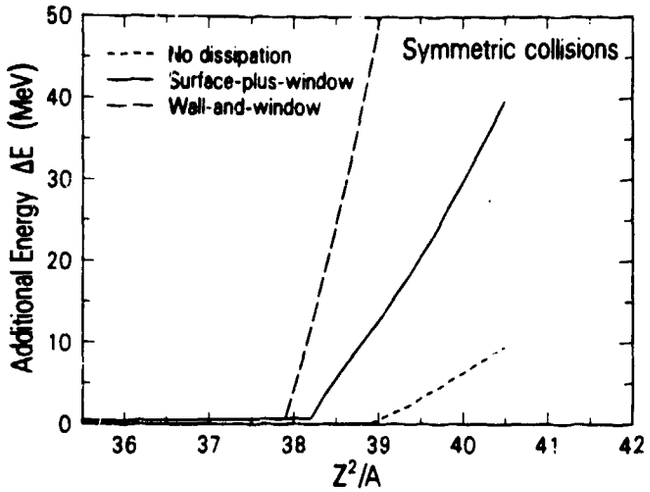

Fig. 6. Effect of dissipation on the additional bombarding energy ΔE required to form a compound nucleus.

the root-mean-square extensions along the symmetry axis of the matter in each portion about its center of mass.[1,33–35]

Our results calculated for no dissipation are shown in the first column of Fig. 4 and by the short-dashed line in Fig. 5. In the absence of dissipation, the time evolution is very rapid and leads to shapes with high-multipole ripples. In this case, only 4 MeV of additional energy is required to form a compound nucleus. As shown in the second column of Fig. 4 and by the solid line in Fig. 5, surface-plus-window dissipation slows down the dynamical evolution and increases to 22 MeV the additional energy that is required to form a compound nucleus. Finally, as shown in the third column of Fig. 4 and by the long-dashed line in Fig. 5, wall-and-window dissipation slows down the dynamical evolution even more and increases to 85 MeV the additional energy that is required to form a compound nucleus.

The dependence of the additional energy ΔE upon the size of the compound nucleus that is formed in symmetric collisions is shown in Fig. 6. For no dissipation, ΔE is zero below the threshold value $(Z^2/A)_{\rm thr} = 38.9$ and then increases slowly with increasing Z^2/A. With dissipation, ΔE is slightly positive for all values of Z^2/A because of the energy dissipated during the approach of the target and projectile prior to their reaching the maximum in the one-dimensional zero-angular-momentum barrier. For surface-plus-window dissipation, the threshold value is lowered to $(Z^2/A)_{\rm thr} = 38.2$, above which ΔE increases rapidly with increasing Z^2/A. Finally, for wall-and-window dissipation, the threshold value is lowered even further to $(Z^2/A)_{\rm thr} = 37.9$, above which ΔE increases very rapidly with increasing Z^2/A.

The large differences between the three curves in Fig. 6 offer the tantalyzing possibility of determining the mechanism and magnitude of nuclear dissipation from comparisons with experimental data. However, because most of the systems that are studied experimentally are asymmetric, it is necessary to either perform calculations for many individual asymmetric systems or to find an appropriate way to scale the results for asymmetric systems into those calculated for symmetric systems.

For surface-plus-window dissipation, we have calculated the additional energy ΔE for mass asymmetry α defined by

$$\alpha = \frac{A_1 - A_2}{A_1 + A_2} \ , \tag{21}$$

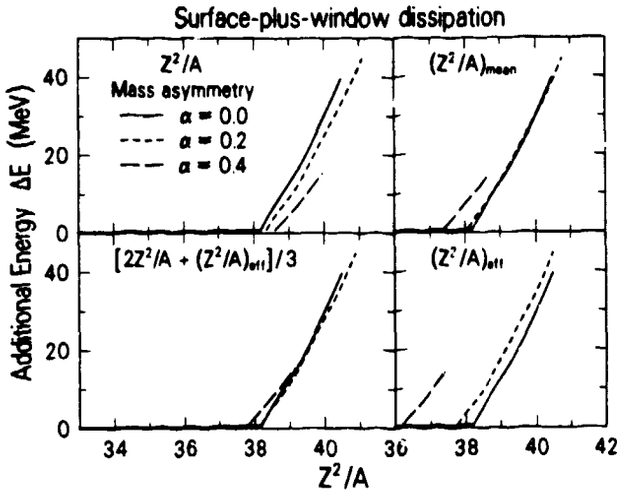

Fig. 7. Search for an appropriate abscissa to scale the results for asymmetric systems into those for symmetric ones.

where A_1 and A_2 are the mass numbers of the target and projectile, respectively. As shown in the upper left-hand portion of Fig. 7, for constant Z^2/A of the compound system, ΔE decreases somewhat with increasing α. On the basis of incoming-channel considerations, it has been suggested that an appropriate scaling abscissa is[9]

$$(Z^2/A)_{\rm eff} = \frac{4Z_1Z_2}{A_1^{1/3}A_2^{1/3}(A_1^{1/3}+A_2^{1/3})} \ , \tag{22}$$

where Z_1 and Z_2 are the atomic numbers of the target and projectile, respectively. However, as shown in the lower right-hand portion of Fig. 7, for constant $(Z^2/A)_{\rm eff}$ of the incoming channel, ΔE increases strongly with increasing α.

Because of the opposite dependence of ΔE on Z^2/A and $(Z^2/A)_{\rm eff}$, the geometric mean[35]

$$(Z^2/A)_{\rm mean} = \left[(Z^2/A)(Z^2/A)_{\rm eff}\right]^{1/2} \tag{23}$$

represents an improved scaling abscissa, as shown in the upper right-hand portion of Fig. 7. However, as shown finally in the lower left-hand portion of Fig. 7, an even better scaling abscissa is the weighted average[12]

$$(Z^2/A)_{\rm wt} = \frac{2}{3}(Z^2/A) + \frac{1}{3}(Z^2/A)_{\rm eff} \ . \tag{24}$$

With this choice of scaling abscissa, we compare in Fig. 8 our results calculated for symmetric systems with experimental values of ΔE derived from various asymmetric systems.[12] The solid circles represent measurements of evaporation residues, and the open circles represent measurements of fission anisotropies. Unlike in the comparisons made in Ref. 12, where the experimental values of ΔE were measured relative to barrier heights calculated by use of the Bass potential,[27] in Fig. 8 the experimental and calculated values of ΔE are both measured relative to barrier heights calculated by use of the Yukawa-plus-exponential potential,[26] with constants determined from a recent nuclear mass formula.[22] For $(Z^2/A)_{\rm wt} \leq 36$, the experimental values of ΔE lie systematically below all three calculated curves by an average of about 3 MeV. This discrepancy could represent an effective lowering of the experimental barrier by zero-point vibrations of the approaching target and projectile, or alternatively could represent a slight deficiency in the values of the constants[22] that are used for the Yukawa-plus-exponential potential.

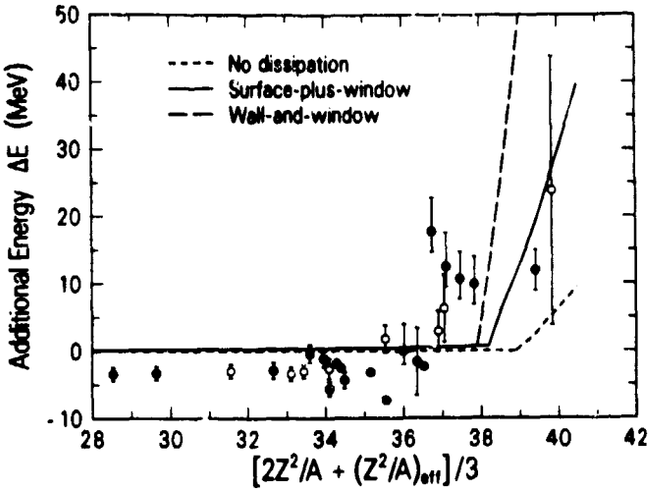

Fig. 8. Comparison of calculated and experimental values of the additional bombarding energy ΔE required to form a compound nucleus.

At $(Z^2/A)_{wt} \approx 37$ the experimental values of ΔE show a rapid rise, as anticipated. However, on a finer scale the trend of the experimental results with $(Z^2/A)_{wt}$ does not follow that predicted by any of the curves. The decreases of ΔE for the four solid circles above the curves as $(Z^2/A)_{wt}$ increases between 36 and 38 is probably associated partly with a change in ground-state shape or stiffness[38] of the ^{90,92,94,96}Zr targets involved. In contrast, the relatively small value of ΔE for the solid circle at $(Z^2/A)_{wt} = 39.4$ probably arises partly from a valley in the potential-energy surface that leads inward from the tangent-sphere configuration for nearly magic target and projectile.[39] While further experimental data that differentiate between shell effects and smooth trends are clearly needed before a definitive conclusion can be drawn from such comparisons, it is apparent that our new surface-plus-window dissipation adequately describes the overall features of experimental dynamical thresholds for compound-nucleus formation.

Surface-plus-window dissipation is also able to describe the enhancement in neutron emission prior to fission that has been observed recently in several heavy-ion-induced reactions. For example, in the reaction $^{16}O + ^{142}Nd \rightarrow ^{158}Er$ at a laboratory bombarding energy of 207 MeV, there are experimentally 2.7 ± 0.4 neutrons emitted prior to fission, compared to 1.6 neutrons calculated with a standard statistical model.[40] An interpretation of this enhancement in terms of neutron emission during the transient time required to build up the quasi-stationary probability flow over the barrier and the mean time required for the system to descend from the saddle point to scission yields an upper limit for the reduced nuclear dissipation coefficient that is consistent with the value calculated for surface-plus-window dissipation.[40]

Finally, we mention tht the widths of mass and charge distributions in deep-inelastic heavy-ion reactions[41] are also adequately described for small energy losses by surface-plus-window dissipation. We have performed no additional calculations in this area, but previous analyses have confirmed the correctness of the window formula.[41] This contribution is carried over essentially unchanged to our new picture, and the calculated widths are insensitive to the strength of the remaining dissipation.

7. Outlook

Nuclear dissipation is a fundamental nuclear property and plays a crucial role in such processes as the production of very heavy elements. Despite much work on its mechanism and magnitude since the 1975 Dubna school-seminar, the emerging theories of dissipation have at times seemed to diverge. Building on the best features of these divergent views, we have presented here a new picture that provides a unified macroscopic description of several diverse nuclear phenomena. These include the widths of isoscalar giant quadrupole and giant octupole resonances, mean fission-fragment kinetic energies and excitation energies, dynamical thresholds for compound-nucleus formation, and widths of mass and charge distributions in deep-inelastic heavy-ion reactions. We hope that our new picture will be subjected to countless experimental tests at Dubna and elsewhere during the coming years.

This work was supported by the U. S. Department of Energy.

References

1. J. R. Nix and A. J. Sierk. *Proc. Int. School-Seminar on Reactions of Heavy Ions with Nuclei and Synthesis of New Elements, Dubna, 1975,* Joint Institute for Nuclear Research Report No. D7-9734 (1976), p. 101.

2. W. J. Swiatecki. *Proc. Int. School-Seminar on Reactions of Heavy Ions with Nuclei and Synthesis of New Elements, Dubna, 1975,* Joint Institute for Nuclear Research Report No. D7-9734 (1976), p. 89.

3. W. J. Swiatecki. *Proc. Int. Conf. on Nuclear Reactions Induced by Heavy Ions, Heidelberg, 1969* (North-Holland, Amsterdam, 1970), p. 729.

4. G. Wegmann. Phys. Lett., **50B** (1974), p. 327.

5. D. H. E. Gross. Nucl. Phys., **A240** (1975), p. 472.

6. J. Błocki, Y. Boneh, J. R. Nix, J. Randrup, M. Robel, A. J. Sierk, and W. J. Swiatecki. Ann. Phys. (N. Y.), **113** (1978), p. 330.

7. J. Randrup and W. J. Swiatecki. Ann. Phys. (N. Y.), **125** (1980), p. 193.

8. W. J. Swiatecki. Prog. Part. Nucl. Phys., **4** (1980), p. 383.

9. W. J. Swiatecki. Phys. Scr., **24** (1981), p. 113.

10. S. Bjørnholm and W. J. Swiatecki. Nucl. Phys., **A391** (1982), p. 471.

11. J. Randrup and W. J. Swiatecki. Nucl. Phys., **A429** (1984), p. 105.

12. J. Błocki, H. Feldmeier, and W. J. Swiatecki. Nucl. Phys., to be published.

13. J. Błocki. These Proceedings.

14. P. Bonche, S. E. Koonin, and J. W. Negele. Phys. Rev., **C13** (1976), p. 1226.

15. J. W. Negele. Rev. Mod. Phys., **54** (1982), p. 913.

16. K. T. R. Davies, K. R. S. Devi, S. E. Koonin, and M. R. Strayer. *Treatise on Heavy-Ion Science, Vol. 3*, edited by D. A. Bromley (Plenum, New York, 1985), p. 3.

17. J. J. Griffin and M. Dworzecka. Nucl. Phys., **A455** (1986), p. 61.

18. C. Yannouleas. Nucl. Phys., **A439** (1985), p. 336.

19. R. W. Hasse and P. Schuck. Nucl. Phys., **A438** (1985), p. 157.

20. J. R. Nix and A. J. Sierk. *Proc. Int. Conf. on Nuclear Physics, Bombay, 1984* (World Scientific, Singapore, 1985), p. 365.

21. J. R. Nix and A. J. Sierk. Phys. Rev., **C21** (1980), p. 396. Phys. Rev., **C25** (1982), p. 1068.

22. P. Möller and J. R. Nix. Nucl. Phys., **A361** (1981), p. 117.

23. M. Aguilar-Benitez *et al.* Phys. Lett., **170B** (1986), p. 1.

24. F. E. Bertrand. Nucl. Phys., **A354** (1981), p. 129c. Private communication (1985).

25. S. Trentalange, S. E. Koonin, and A. J. Sierk. Phys. Rev., **C22** (1980), p. 1159.

26. H. J. Krappe, J. R. Nix, and A. J. Sierk. Phys. Rev., **C20** (1979), p. 992.

27. J. Kunz and J. R. Nix. Z. Phys., **A321** (1985), p. 455.

28. J. R. Nix. Nucl. Phys., **A130** (1969), p. 241.

29. J. R. Nix, A. J. Sierk, H. Hofmann, F. Scheuter, and D. Vautherin. Nucl. Phys., **A424** (1984), p. 239.

30. P. Grangé, J. Q. Li, and H. A. Weidenmüller. Phys. Rev., **C27** (1933), p. 2063.

31. F. Scheuter, C. Grégoire, H. Hofmann, and J. R. Nix. Phys. Lett., **149B** (1984), p. 303.

32. A. E. S. Green. *Nuclear Physics* (McGraw-Hill, New York, 1955), pp. 185, 250.

33. A. J. Sierk and J. R. Nix. *Proc. Third IAEA Symp. on the Physics and Chemistry of Fission, Rochester, 1973, Vol. II* (International Atomic Energy Agency, Vienna, 1974), p. 273.

34. J. R. Nix and A. J. Sierk. Phys. Rev., **C15** (1977), p. 2072.

35. K. T. R. Davies, A. J. Sierk, and J. R. Nix. Phys. Rev., **C28** (1983), p. 679.

36. J. Randrup. Ann. Phys. (N. Y.), **112** (1978), p. 356.

37. R. Bass. *Proc. Symp. on Deep-Inelastic and Fusion Reactions with Heavy Ions, Berlin, 1979* (Springer-Verlag, Berlin, 1980), p. 281.

38. R. Bengtsson, P. Möller, J. R. Nix, and J. Y. Zhang. Phys. Scr., **29** (1984), p. 402.

39. P. Möller, J. R. Nix, and W. J. Swiatecki. These Proceedings. Nucl. Phys., to be published.

40. P. Grangé, S. Hassani, H. A. Weidenmüller, A. Gavron, J. R. Nix, and A. J. Sierk. Phys. Rev., **C34** (1986), p. 209.

41. W. U. Schröder and J. R. Huizenga. *Treatise on Heavy-Ion Science, Vol. 2*, edited by D. A. Bromley (Plenum, New York, 1984), p. 115.